STUDIA UNIVERSITATIS BABEŞ-BOLYAI, CHEMIA, LII, 3, 2007

ON THE DYNAMICS OF FREE DROPS

MARIA TOMOAIA-COTISEL[a], EUGENIA GAVRILA[a], IOSIF ALBU[a] AND IOAN-RĂDUCAN STAN[b]

ABSTRACT. This is a review on the original work by *Chifu et al.* that explored the various movements of the free drops. This review also presents some theoretical models and experiments further developed by *the academic research group, established by him in the physical chemistry department*, to deeply investigate the free drop dynamics and related interfacial phenomena. The interfacial tension gradient caused by the surfactant adsorption at the surface of a free liquid drop gives rise to a surface flow (i.e. Marangoni interfacial flow) which causes the motion of the neighboring liquids by viscous traction, and generates a hydrodynamic pressure force, named Marangoni force, which acts on the drop surface. The effect of the surfactant adsorption and of Marangoni force on the dynamics of free liquid drops immersed in an unbounded liquid (the densities of the two bulk liquids are equal) is studied. Marangoni force was examined on several cases using non-deformable and deformable free drops. For a low value of the viscosity ratio of the two liquids (i.e., the drop liquid viscosity /unbounded liquid viscosity) at a high interfacial tension gradient, a dynamic instability of the drop was experimentally observed. This instability once triggered develops into the fragmentation of the drop into two droplets. For high values of the viscosity ratio of the two bulk liquids at a high interfacial tension gradient, only drop deformations appear. In the situation of a very high viscosity ratio and at a small interfacial tension gradient the drops are undeformable. The observed experimental data are in a substantial agreement with the results of our hydrodynamic theoretical model.

Keywords: Marangoni force, Marangoni effect, free drop deformations, interfacial tension gradient, drop dynamics, hydrodynamic model

INTRODUCTION

Since the original work by Chifu et al. [1-3] that describes the dynamics of a free liquid drop, immersed in an equal density bulk liquid, when a surface tension gradient is applied on the drop surface, some theoretical models and experiments were further developed to explore the drop dynamics [4-9]. To explain the drop dynamics, it was suggested that Marangoni instability, surface dilution, tip-stretching and capillary forces are important factors in drop movements and deformations.

[a] Babes-Bolyai University of Cluj-Napoca, Department of Physical Chemistry, Arany Janos Str., No. 11, 400028 Cluj-Napoca, Romania;
[b] Babes-Bolyai University of Cluj- Napoca, Department of Mechanics and Astronomy, Kogalniceanu Str., No. 1, 400084 Cluj-Napoca, Romania e-mail: mcotisel@yahoo.com, i_r_stan@yahoo.com

To determine which one from these is a major factor on the drop dynamics, in this work, we investigate experimentally and theoretically the effect of local changes in the surface tension, which are induced by the adsorption of a surfactant at the drop surface.

As a result of the adsorption of a surfactant (also called surface active compound), a surface tension gradient (Marangoni effect) appears, which generates a real surface flow, from low to high surface tension, called the Marangoni flow, and it is illustrated in Fig. 1. This Marangoni interfacial flow causes the motion of the neighboring liquids by viscous traction [3, 5], and generates the force of hydrodynamic pressure, named Marangoni force, which acts on the drop surface.

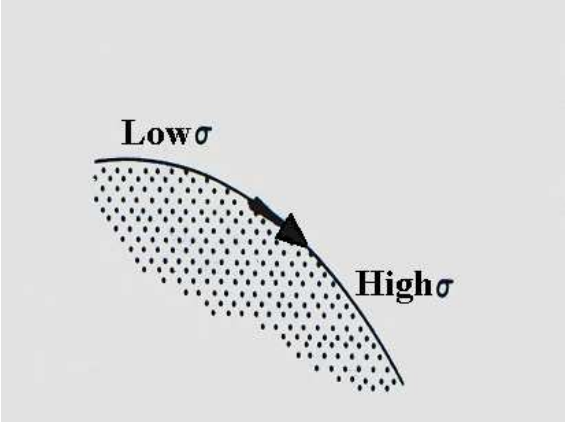

Fig.1. Marangoni interfacial flow resulting under a surface tension gradient

In this work, we have also developed a theoretical hydrodynamic model to calculate the Marangoni force. At the beginning of the interfacial flow, the Marangoni force acts like a “hammer” and modifies the shape of the drop. This force also generates other various factors, like the surface dilution, the tip-stretching, and the capillary forces, that might appear in the drop dynamics, depending on the working conditions. The results of our theoretical hydrodynamic model are in a substantial agreement with the observed experimental data.

THEORY

The investigation of the free drop dynamics is of a present interest, due to its appearance both in the industrial and biological processes, as well as in the space science and technology of liquids.

Hydrodynamic governing equations

We consider a viscous (L') liquid drop (with density ρ') immersed in an unbounded immiscible (L) liquid (of density ρ) at a constant temperature (T). The densities of the two bulk liquids are equal (ρ = ρ') and initially the drop is motionless. Such a drop is also called free drop.

Further, we assume that both liquids (L and L') are incompressible and Newtonian. The drop has a viscosity μ' and the surrounding bulk fluid a viscosity μ, which are, in general, different. The surface between the two bulk fluids is characterized by an interfacial tension noted σ_0.

Then, a small quantity of a surfactant (e.g. a droplet of 10^{-3}-10^{-2} cm^3, which is very small compared with the volume of the initial drop) is introduced on a well-chosen point (called also injection point) at the drop surface.

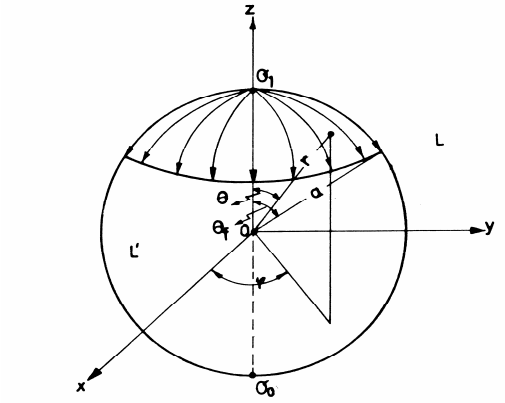

Fig. 2. The spreading and adsorption of a surfactant on the drop surface; the system of spherical coordinates (r, θ, φ); the θ_f angle characterizes the position of the surfactant front.

The surfactant, because of its molecular structure, is spread and simultaneously adsorbed at the liquid-liquid interface and it is continuously swept along the meridians of the drop by the convective transport (see, Fig. 2). In the injection point the interfacial tension is instantaneously lowered to σ_1 value. We mention that local changes in temperature [8] or the presence of surface chemical reactions might produce a similar effect.

Since the interfacial tension is a function of the surfactant concentration, a gradient of interfacial tension is established over the surface of the drop [3]. Consequently, the Marangoni spreading of the surfactant takes place from low surface tension to high surface tension (Fig. 1). As a result of the Marangoni surface flow, which causes the motion of the neighboring liquids by viscous traction, the Marangoni force of hydrodynamic pressure will appear acting on the

drop surface. Due to the drop symmetry, the Marangoni force has the application point in the injection point with surfactant at the drop surface.

This Marangoni force will determine all kinds of drop movements, especially deformations, rotations and oscillations of the whole drop, as well as surface waves and drop translational motions depending on the experimental working conditions.

The symmetry of the problem suggests a system of spherical coordinates (r, θ, φ) with the origin placed in the drop center and with the Oz axis passing through the sphere in the point of the minimum interfacial tension, i. e. the injection point of the surfactant.

We underline that the surfactant injection point at the drop surface may be taken anywhere, the drop being initially at rest. In the following theoretical model, we shall take it like it is shown in Fig. 2.

The surfactant front position, in this radial flow, is noted by the angle θ_f. and the interfacial tension, σ, is considered a unique function of the angle θ. Within the surfactant invaded region, ($0 \le \theta \le \theta_f$), for the variation of the interfacial tension [5] with θ, we take

$$\sigma(\theta) = \frac{\sigma_0 - \sigma_1}{1 - \cos\theta_f}(1 - \cos\theta) + \sigma_1 \qquad (1)$$

where $\sigma_0 = \sigma(\theta_f)$ and $\sigma_1 = \sigma(0)$.

Derivation of Eq. (1) gives the interfacial tension gradient in the invaded drop region with surfactant

$$\frac{d\sigma}{d\theta} = \frac{\sigma_0 - \sigma_1}{1 - \cos\theta_f}\sin\theta, \qquad (2)$$

where, the interfacial tension σ_0 is constant in any point of the uncovered surface, while the interfacial tension difference $\Pi = \sigma_0 - \sigma_1$ arises only in the invaded region. It is clear that only σ_1 and σ_0, i. e. the minimum and the maximum values of the interfacial tension, can be experimentally measured.

From the theoretical point of view, the variation of the interfacial tension σ(θ) with the angle θ, inside the invaded region, is of the following form $\sigma(\theta) = \sigma_m + a_1 \cos\theta$ where σ_m and a_1 have different expressions. For the particular case when the surface of the entire drop is covered with surfactant $\theta_f = \pi$, the equation obtained is similar to that proposed by other authors [10].

The equations, governing the flow inside and outside the drop, are the continuity and Navier-Stokes equations [11-13]. The continuity equations for a Newtonian incompressible fluid are

$$\text{div } \vec{v} = 0 , \tag{3}$$

$$\text{div } \vec{v}' = 0 , \tag{4}$$

where $\vec{v}$ is the velocity of the bulk liquid L and $\vec{v}$' represents the velocity of the liquid L' within the drop.

The Navier - Stokes equations for a steady flow are :

$$(\vec{v} \cdot \nabla)\, \vec{v} = -\frac{1}{\rho} \text{grad } p + \nu \Delta \vec{v}, \tag{5}$$

$$(\vec{v}' \cdot \nabla)\, \vec{v}' = -\frac{1}{\rho} \text{grad } p' + \nu' \Delta \vec{v}', \tag{6}$$

where p and p' are the pressures outside and inside of the drop; $\nu = \frac{\mu}{\rho}$ and $\nu' = \frac{\mu'}{\rho}$ are the kinematic viscosities of continuous liquid and drop liquid, respectively. All these parameters are considered constants.

We give here some account on the equations governing fluid motion in a surface or in an interface, which is considered a two dimensional, incompressible Newtonian fluid, having surface density Γ and surface dilatational κ and shear ε viscosity. Even that we consider the interface like a two-dimensional geometrical surface, it has a thickness about 5.10^{-10} cm.

The flow in a surface is not just a flow in a two-dimensional space whose governing equations will be immediate analogs of the three-dimensional ones. In contrast with the three- dimensional space, this surface is a two-dimensional space that moves within a three-dimensional space surrounding it. In our case, the interface is the region of contact of two liquids, i.e. drop liquid and bulk liquid. This is a new feature which oblige us to take account on the dynamical connection between the surface and its surroundings, namely on the traction exerted by the outer $\vec{T}$ and inner $\vec{T}'$ liquid upon the drop interface.

The equation of the interfacial flow [14 - 16] is

$$\Gamma\left(\vec{w} \cdot \nabla_S\right) \vec{w} = \vec{F} + \nabla_S \sigma + \left(\kappa + \varepsilon\right) \nabla_S \left(\nabla_S \cdot \vec{w}\right), \tag{7}$$

where $\vec{w} = \vec{v}_S$ is the interface velocity, $\vec{F} = \Gamma \vec{g} + \vec{T} - \vec{T}'$ is the external force acting on the drop surface, and ∇_S is the surface gradient operator.

Because the surface density [16] is very small ($\Gamma \approx 10^{-7}$g cm^{-2}) the inertial term can be neglected against the remainder terms.

It is significant to underline that equation (7) can be used in two ways: as the equation which describes the surface flow or as a dynamical boundary condition.

In order to find the distributions of the velocities $\vec{v}$ and $\vec{v}'$ and of the pressures p and p', the system of equations (3)-(7) must be solved taking into account some appropriate boundary conditions [11- 13].

Thus, the velocities of the inner and outer liquid of the drop must satisfy the following conditions:

- the outer velocity must be zero far from the drop surface,

$$\vec{v} = 0 \quad \text{for } r \to \infty ;$$

- the normal component of the outer and the inner velocities must be zero on the surface of the drop

$$\vec{v}_n = \vec{v}_n' = 0 , \quad \text{at} \quad r = a;$$

- the tangential velocity components of the two liquids at the interface must be equals

$$\vec{v}_t = \vec{v}_t' \qquad \text{at} \quad r = a;$$

- the velocity $\vec{v}$ within the drop must remain finite at all points, particularly at the centre of the drop (r = 0 the origin of the coordinates).

Since the Marangoni flow on the surface of the drop r = a is symmetrical with respect to the Oz axis, the velocities of the inner and outer liquid flows are not functions of the angle φ, they will have only normal (radial) and tangential components $v_r(r,\theta), v_r'(r,\theta), v_\theta(r,\theta), v_\theta'(r,\theta)$.

The continuity equation (3) for the outer flow in spherical coordinates is

$$\frac{\partial v_r}{\partial r} + \frac{1}{r}\frac{\partial v_\theta}{\partial \theta} + \frac{2v_r}{r} + \frac{v_\theta \operatorname{ctq}\theta}{r} = 0, \tag{8}$$

while for the Navier-Stokes equation (5) we have

$$\frac{\partial p}{\partial r} = \mu\left(\frac{\partial^2 v_r}{\partial r^2} + \frac{1}{r^2}\frac{\partial^2 v_r}{\partial \theta^2} + \frac{2}{r}\frac{\partial v_r}{\partial r} + \frac{\operatorname{ctg}\theta}{r^2}\frac{\partial v_r}{\partial \theta} - \frac{2}{r^2}\frac{\partial v_\theta}{\partial \theta} - \frac{2v_r}{r^2} - \frac{2\operatorname{ctg}\theta}{r^2}v_\theta\right) \tag{9}$$

$$\frac{1}{r}\frac{\partial p}{\partial \theta} = \mu\left(\frac{\partial^2 v_\theta}{\partial r^2} + \frac{1}{r^2}\frac{\partial^2 v_\theta}{\partial \theta^2} + \frac{2}{r}\frac{\partial v_\theta}{\partial r} + \frac{ctg\,\theta}{r^2}\frac{\partial v_\theta}{\partial \theta} + \frac{2}{r^2}\frac{\partial v_r}{\partial \theta} - \frac{v_\theta}{r^2 \sin^2\theta}\right) \quad (10)$$

It is to be noted that similar equations are obtained for the inner liquid motion.

The velocities of the inner and outer flow satisfy the following boundary conditions

$$v_r = v_\theta = 0 \quad \text{for} \quad r \to \infty, \quad (11)$$

$$v_r = v_r' = 0 \text{ at } r = a, \quad (12)$$

$$v_\theta = v_\theta' \qquad \text{at} \quad r = a \ , \quad (13)$$

$$v_r' \text{ and } v_\theta' \quad \text{finite at} \quad r = 0 \ . \quad (14)$$

In addition to these kinematic conditions we also have, as we pointed before, a dynamic condition on the drop surface (r = a), obtained from the interface flow equation (7), which for small interfacial density Γ can be written in the following form [14, 15]:

$$\mu\left(\frac{1}{r}\frac{\partial v_r}{\partial \theta} + \frac{\partial v_\theta}{\partial r} - \frac{v_\theta}{r}\right)_{r=a} + \frac{1}{a}\frac{d\sigma}{d\theta} + (\kappa + \varepsilon)\left[\frac{1}{r}\frac{\partial}{\partial \theta}\left\{\frac{1}{r\sin\theta}\frac{\partial}{\partial \theta}(v_\theta \sin\theta)\right\}\right]_{r=a} \quad (15)$$
$$+ \varepsilon\frac{2(v_\theta)_{r=a}}{a^2} = \mu'\left(\frac{1}{r}\frac{\partial v_r'}{\partial \theta} + \frac{\partial v_\theta'}{\partial r} - \frac{v_\theta'}{r}\right)_{r=a}$$

Solution of the flow equations

The solution of the flow equations (8-10) with the boundary conditions (11-15) can be obtained if we note that the surface flow gives rise to a current fluid directed to the drop along the Oz axis. This current fluid arises as a consequence of the continual replacement, by a ventilation effect, of that liquid layer which it was displaced by the interfacial flow. The profile of the flow indicates that a solution of the flow equations should be sought [13, 17] in the form

$$v_r(r,\theta) = f(r)\cos\theta,$$
$$v_\theta(r,\theta) = g(r)\sin\theta,$$
$$p(r,\theta) = \mu\, h(r)\cos\theta,$$

for the outer liquid L, and similar Eqs. are obtained for the inner liquid L'.

After well-known manipulations [17] we obtain for f, g, and h the following relations:

$$f(r) = \frac{b_1}{r^3} + \frac{b_2}{r} + b_3 + b_4 r^2,$$

$$g(r) = \frac{b_1}{2r^3} - \frac{b_2}{2r} - b_3 - 2b_4 r^2,$$

$$h(r) = \frac{b_2}{r} + 10 b_4 r,$$

with b_1, b_2, b_3 and b_4 as constants. Also, equations of identical form for f', g' and h' are obtained with constants b_1', b_2', b_3', b_4'.

The eight b unknown constants will be determined from the boundary conditions (11-15). From (11) and (14) we have $b_3 = b_4 = b_1' = b_2' = 0$. For the outer liquid motion we obtain:

$$v_r(r,\theta) = \left(\frac{b_1}{r^3} + \frac{b_2}{r} \right) \cos\theta,$$

$$v_\theta(r,\theta) = \left(\frac{b_1}{2r^3} - \frac{b_2}{2r} \right) \sin\theta,$$

$$p(r,\theta) = \mu \frac{b_2}{r^2} \cos\theta,$$

and for the velocity and pressure distribution within the drop

$$v_r'(r,\theta) = (b_3' r^2 + b_4') \cos\theta,$$

$$v_\theta'(r,\theta) = -(2b_3' r^2 + b_4') \sin\theta,$$

$$p'(r,\theta) = 10\mu' b_3' r \cos\theta.$$

From (12) and (13) we have

$$b_2 = -\frac{b_1}{a^2}, \quad b_3' = -\frac{b_1}{a^5}, \quad b_4' = \frac{b_1}{a^3}.$$

Then, from equation (15), where for $\frac{d\sigma}{d\theta}$ we have used equation (2), the dependence of the constant b_1 as a function of the interfacial tension gradient $\Pi = \sigma_0 - \sigma_1$ is obtained:

$$b_1 = \frac{(\sigma_0 - \sigma_1)a^3}{3(\mu + \mu' + 2\kappa/3a)(1 - \cos\theta_f)} .$$

Thus, Eqs. (8-10) with the appropriate boundary conditions (11-15) lead to the distribution of the velocities $\vec{v}, \vec{v}'$ and of the pressures p, p' outside and inside the drop:

$$v_r(r,\theta) = \frac{(\sigma_0 - \sigma_1)a^3}{3(\mu + \mu' + 2\kappa/3a)(1 - \cos\theta_f)}\left(\frac{1}{r^3} - \frac{1}{a^2 r}\right)\cos\theta, \tag{16}$$

$$v_\theta(r,\theta) = \frac{(\sigma_0 - \sigma_1)a^3}{3(\mu + \mu' + 2\kappa/3a)(1 - \cos\theta_f)}\left(\frac{1}{2r^3} + \frac{1}{2a^2 r}\right)\sin\theta, \tag{17}$$

$$p(r,\theta) = -\frac{\mu(\sigma_0 - \sigma_1)\,a}{3r^2(\mu + \mu' + 2\kappa/3a)(1 - \cos\theta_f)}\cos\theta, \tag{18}$$

for the outer flow, and

$$v_r'(r,\theta) = \frac{\sigma_0 - \sigma_1}{3(\mu + \mu' + 2\kappa/3a)(1 - \cos\theta_f)}\left(1 - \frac{r^2}{a^2}\right)\cos\theta \tag{19}$$

$$v_\theta'(r,\theta) = -\frac{\sigma_0 - \sigma_1}{3(\mu + \mu' + 2\kappa/3a)(1 - \cos\theta_f)}\left(1 - \frac{2r^2}{a^2}\right)\sin\theta \tag{20}$$

$$p'(r,\theta) = -\frac{10\,\mu'(\sigma_0 - \sigma_1)r}{3\,a^2(\mu + \mu' + 2\kappa/3a)(1 - \cos\theta_f)}\cos\theta \tag{21}$$

for the inner flow.

Marangoni force F_M exerted on the drop

Further, we describe the Marangoni force exerted on the free drop due to Marangoni flow. If we analyze the model of the Marangoni interfacial flow, we find that as the flow occurs with the driving by viscosity of the outer

liquid L, forces of hydrodynamic pressure will act on the drop L'. The resultant F_M, of the forces exerted by the fluid on the drop, due to the symmetry of the Marangoni flow, is oriented along the Oz axis. Is has been computed by integrating the surface forces [11] acting along the drop surface:

$$F_M = \iint_S (p_{rr}\cos\theta - p_{r\theta}\sin\theta)\, ds \tag{22}$$

where, ds is the surface element covered with surfactant, and p_{rr} and $p_{r\theta}$ are the normal and tangential components [11-13], respectively, of the viscous stress tensor given by:

$$p_{rr}(r,\theta) = -p + 2\mu\frac{\partial v_r}{\partial r}, \tag{23}$$

$$p_{r\theta}(r,\theta) = \mu\left(\frac{1}{r}\frac{\partial v_r}{\partial \theta} + \frac{\partial v_\theta}{\partial r} - \frac{v_\theta}{r}\right). \tag{24}$$

The surface element in spherical coordinates on the drop (r = a) is

$$ds = 2\pi a^2 \sin\theta\, d\theta,$$

and, the force acting on the drop, given by (Eq. (22), can then be rewritten as:

$$F_M(\theta_f) = 2\pi a^2 \int_0^{\theta_f} (p_{rr}\cos\theta - p_{r\theta}\sin\theta)\sin\theta\, d\theta\,. \tag{25}$$

Using Eqs. (16-18), one obtains for the normal (Eq. (23) and tangential components (Eq. (24)) of the stress tensor, at the drop surface (r = a), the following expressions:

$$(p_{rr})_{r=a} = -\frac{\mu(\sigma_0 - \sigma_1)}{a\left(\mu + \mu' + 2\kappa/3a\right)(1-\cos\theta_f)}\cos\theta, \tag{26}$$

$$(p_{r\theta})_{r=a} = -\frac{\mu(\sigma_0 - \sigma_1)}{a\left(\mu + \mu' + 2\kappa/3a\right)(1-\cos\theta_f)}\sin\theta\,. \tag{27}$$

Introducing the viscosities ratio, $\lambda = \mu'/\mu$, the interfacial tension difference, $\Pi = \sigma_0 - \sigma_1$ and because $2\kappa/3a \approx 0$ as shown previously [5], after integration we have:

$$F_M(\theta_f) = A\,(1- 2\cos\theta_f - 2\cos^2\theta_f), \qquad (28)$$

where A is given by

$$A=\frac{2\pi a\,\Pi}{1+\lambda}\ .$$

Thus, Eq. (28) represents the Marangoni force acting on the drop surface along the Oz axis. It can be seen that this force depends on the θ_f angle, namely, on the extent to which the drop surface is covered by the surfactant, as a function of the radial interfacial tension difference (Π), the ratio of the bulk viscosities (λ), as well as of the radius (a) of the drop.

Hammer Effect

For further discussions, it is useful to introduce a new function in Eq. (28), namely $f(\theta_f)= F_M(\theta_f)/A$, given by:

$$f(\theta_f) = 1-2\cos\theta_f -2\cos^2\theta_f \qquad (29)$$

which is plotted in Fig. 3.

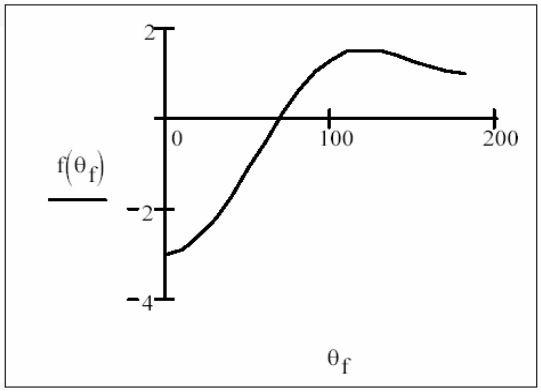

Fig. 3. The graphic of $f(\theta_f)$ as a function of θ_f angle

The value of θ_f, for which the force $F_M(\theta_f)$ cancels, $F_M(\theta_f) = 0$, is $\theta_0 \approx 68.53^0$. The value of θ_0 does not depend on the physical, chemical and geometric properties of the drop. Also, we see that for $\theta_f \in [0,\theta_0)$, the force is negative $F_M(\theta_f) <0$, and for $\theta_f \in (\theta_0, 180^0]$ the force is positive, $F_M(\theta_f)> 0$, having the greatest value for $\theta_m = 120^0$.

From Eq. (28) it is found that for a coverage degree $\theta_f < \theta_0$ of the drop, with surfactant, as a result of the appearance of a radial interfacial tension gradient Π, the pressure force $F_M(\theta_f)$ exerted by the external liquid upon the drop is oriented toward the negative direction of the Oz axis (Fig. 3). This is similar with the application of a "hammer" knock on the drop in the injecting point of the surfactant. For a coverage degree θ_f greater than θ_0, but less than 180^0, the force $F_M(\theta_f)$ is oriented towards the positive direction of the Oz axis. The propulsive (lifting) force, $F_M(\theta_f) > 0$, responsible for the upward movement of the drop, appears only when the coverage of the drop with surfactant is greater than θ_0.

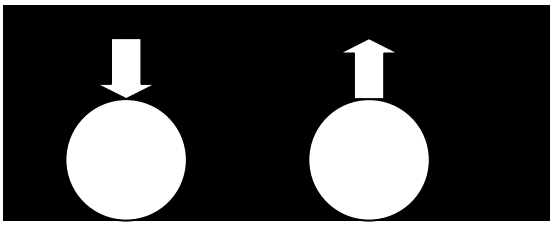

(a) (b)

Fig. 4. The Marangoni force, F_M, acting on the free drop.
a) Marangoni hammer force; b) Marangoni lifting force.

Therefore, the effect of coverage by the surfactant on the drop surface can be decomposed in two parts, the "hammer" effect for the coverage $0 \le \theta_f < \theta_0$ and the "propulsive" effect for the coverage $\theta_0 < \theta_f \le 180^0$ as shown in Fig.4a and 4b, respectively.

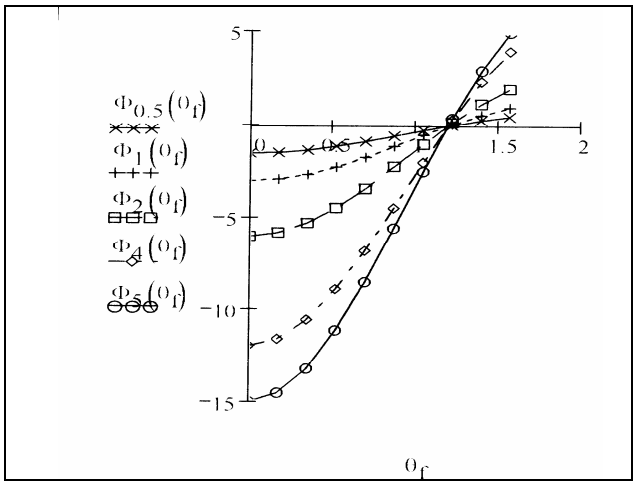

Fig.5. The plot of $\Phi_\Pi(\theta_f)$ versus θ_f, for $\theta_f < \theta_0$

To point out the role of the surface tension effects on the F_M force in the hammer case $\theta_f < \theta_0$ we introduce, in Eq. (28), another new function $\Phi_\Pi = \Pi\, f(\theta_f)$.

This Φ_Π function is a reduced Marangoni hydrodynamic force. Its graphic representation, Φ_Π versus θ_f, for various chosen values of Π (e.g., 0.5; 1; 2; 4; and 5 dyn/cm) is given in Fig.5.

It is observed that for high surface tension differences (e.g., 4 dyn/cm and 5 dyn/cm) the "hammer" effect is also high. For low surface tension differences (e.g. 0.5 dyn/cm, 1 dyn/cm and 2 dyn/cm), the hammer effect is small. This result is in good agreement with our previous work [3, 17], where the main goal was to maintain the drop non-deformable using high viscosity liquids and small surface tension gradients.

The F_M (θ_f) force reaches its maximum value at the spreading moment of the surfactant (t=0) for which $\theta_f \approx 0$ and is given by:

$$F(0) = \frac{6\pi\, a\, \Pi}{1+\lambda}, \tag{30}$$

where F(0) represents the resultant force acting on the drop surface in the injecting point. For physical meanings, we can take the absolute value of this Marangoni hammer force.

Drop deformation

In our opinion, the Marangoni hammer force is the principal factor which can modify the shape of the drop, namely through deformations and break-ups of a drop. To see how this Marangoni force works, we give in Table 1 the values of the ratio F_M (θ_f) /*A* for different values of the θ_f.

Table 1.

The values of F_M (θ_f) /*A* are given versus θ_f

θ_f	0^0	10^0	20^0	30^0	40^0	50^0	60^0	68.53^0
F_M/A	-3	- 2.91	- 2.65	-2.23	- 1.70	-1.12	-0.50	0

In Fig. 6, we plotted the Marangoni hammer forces acting on the drop surface for different θ_f values, which are belonging to the interval of $[-\theta_0, +\theta_0]$.

Fig. 6 suggests that it is a direct connection between Marangoni hammer force $F_M(\theta_f)$ and the drop deformation, namely along the Oz axis. Our experiments confirmed this supposition in both cases, for the deformation and for break-up.

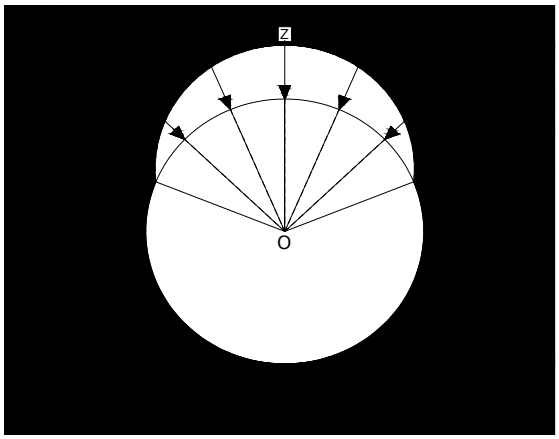

Fig. 6. Marangoni hammer forces acting on a free drop surface

We wish to point out the importance of this Marangoni hammer force, which is at the origin of other processes [18-23]. Indeed, the modification of the surface area of a drop, when the drop is deformed to a non-spherical shape, dilutes the surfactant surface concentration and the deformation of the drop is different from that expected one for the equilibrium σ_0 case. This is called the surface dilution effect.

Also, especially at the break-up process of the drop, surfactant molecules may accumulate at the tip of the drop due to the convection phenomenon. This phenomenon decreases the local interfacial tension and causes the tip to be overstretched. This process is called the tip-stretched effect. When during the deformations, a drop gets a concave surface, capillary forces appear, which tend to bring the drop in the initial spherical shape. All these effects appear, in our opinion, as a consequence of the Marangoni hammer force and of the real flow of the surfactant molecules within the drop surface.

Therefore, we suggest that the primary effect, due to a reduction of the equilibrium interfacial tension (σ_0) in the injection point of a free drop surface with a surfactant, at *t=0,* is the appearance of a Marangoni surface flow of the surfactant on the drop surface. This Marangoni flow of the surfactant modifies the equilibrium surface tension, σ_0, and a Marangoni force $F_M(\theta_f)$ will act on the drop. At the beginning, it acts like a hammer which changes the shape of the drop, and consequently, several factors might appear, namely, the surface dilution and tip-stretching, as well as capillary forces.

Internal wave trains.

Further, we suggest that it is a direct connection between Marangoni force and the deformation of the drop, via the surface waves produced by the hammer effect.

Furthermore, we have considered that the surface waves, generated by the hammer effect, produce traveling periodic internal wave trains (Fig. 7). If these internal waves are absorbed by drop, the shape of the drop is not deformed. If these internal waves are not absorbed, the overlapping of the direct and reflected internal waves modifies the shape of the drop and causes deformations or even the break-up of the drop.

For small surface tension gradients, even in the case of the drop not deformable, there are different movements, first of all, the surface waves. We suggest that these surface waves are produced by the hammer effect described above. The surface waves generate a surface Marangoni instability of the drop. This instability was observed previously [23] but its cause was not discovered.

Our theoretical model can describe the surface instability due to the hammer effect. Further on, these surface waves will produce the internal waves (Fig. 7) which are generated by the surface tension gradients through hammer impact. As a consequence, traveling periodic internal wave trains are generated in the liquid drop after the adsorption and spreading of the surface-active compound on the surface of the drop, as illustrated latter on in the experimental work.

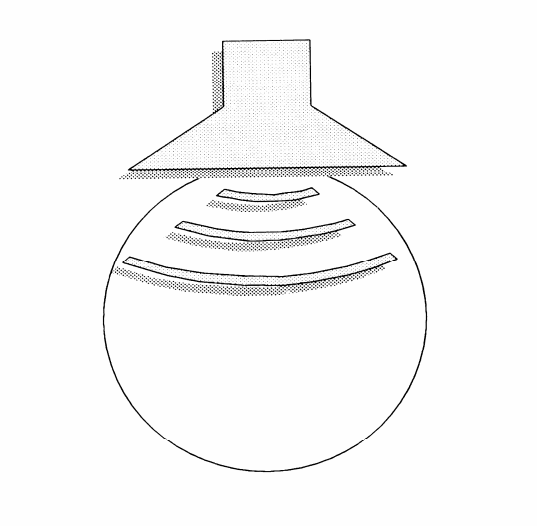

Fig. 7. Internal wave trains

Further more, two possibilities can occur for the hammer effect ($\theta_f \leq \theta_0$):

1. If the drop viscosity μ' is large, then, the energy of the traveling periodic internal trains of waves are absorbed by the drop liquid and the drop is not deformable. Nevertheless, other movements might appear, like oscillations of the whole drop and rotations.
2. When the drop viscosity μ' is small and the energy of the internal waves is not absorbed and the waves are reflected by the internal

drop surface. The superimposing of the direct internal waves with the reflected ones gives rise to a “resonant” effect, which generates the deformation and even break-up of the drop.

EXPERIMENTAL SECTION

The experimental work on drop dynamics and Marangoni instability was performed in liquid-liquid systems of equal densities presented in Tables 2 and 3. The densities of the liquids were determined picnometrically and the bulk viscosities by using an Ubbelhode viscometer. The surface dilatation viscosity at the liquid/liquid interface was not directly measured and only a few indications concerning this magnitude for the liquid/gas interface have been found [3].

The mixtures, making up the continuous L phase, were placed in a thermostated parallelepipedic vessel of 1 dm^3, made of transparent glass. The drop (L’) was made of various radii between 0.46 and 1.19 cm, by using the mixtures described in Table 2. The L’ liquid was carefully submerged by using a pipette into the continuous L aqueous phase and the density of the latter was then adjusted by adding small quantities of water or alcohol until the buoyancy of the drop practically disappeared.

After the system was stabilized, a small quantity (10^{-3}-10^{-2} cm^3) of the surfactant solution (S) was injected with a micrometric syringe, in a point on the drop surface (injection point in Fig, 2). The injection was done either in a vertical direction (as in Fig. 8) or in different directions (Figs 9 and 10) and no influence of the mode of injection on the Marangoni flow or on the drop movements and deformations were observed.

The interfacial tension for the liquid/liquid systems, e.g. L/L’ and L’/S, was determined by a method based on capillarity [3] and its value is given in Table 2. The measurement of the above parameters as well as the drop dynamics and surface flow experiments have been performed at constant temperature (20 $\pm$ 0.1^oC). All chemicals were of analytical purity and used without further purification. In order to make visible the surface flow, the surfactant solution was intensely colored with methylene blue (0.28 g/100 cm^3). We mention that we used surfactants which were soluble in the continuous phase L for systems 1 and 2. For the 3 – 6 systems, the surfactant was insoluble both in the L and L’ liquid phases.

The movement of the surfactant front was followed by filming with a high speed camera (500 images/sec). A number of sequences, showing the surfactant front position at various moments t of the process, is presented in Fig. 8. It can be seen that the front position is easily distinguishable from the uncovered drop surface.

The positioning of the L’ liquid drop in the continuous L liquid for a sufficiently long time as to perform the flow measurements raises difficulties. Although some authors pointed out that two drops never behave in the same manner under the action of interfacial tension differences, we have succeeded

in measuring the reproducible surface flow velocities as well as in evidencing the influence of several factors, like interfacial tension gradients and viscosities, on the drop deformations and movements. Several examples will be presented in the next section.

RESULTS AND DISCUSSION

Table 2.

Composition and physical characteristics of the liquid/liquid systems of equal densities. For systems 3 to 5, the composition of phase L is given in (% of weight). For bulk viscosities μ and μ', and interfacial tensions σ_0 and σ_1, see the text. For systems 1 and 2, the drop radius is a = 1.19 cm and for systems 3 to 6, the drop radius is a = 0.46 cm.

System No.	Continuous Phase (**L**)			Drop Phase (**L'**)		Surfactant Solution (**S**)	
	Composition (% vol)	μ(cP)	σ_0 **L / L'** (dyn/cm)	Composition (% vol)	μ'(cP)	Composition (% vol)	σ_1 **L' / S** (dyn/ cm)
1	Ethanol 78.6 Water 21.4	2.26	7.9	Paraffin oil	80	Propanol 77.3 Water 22.7	3.5
2	Methanol 78 Water 22	1.33	10.2	Paraffin oil	80	Propanol 77.3 Water 22.7	3.5
3	$NaNO_3$ 15.1 Water 84.9	1.1	28.7	Chlor benzene 40 Silicon oil 60	8. 04	Benzylic alcohol 89 CCl_4 11	3.6
4	$NaNO_3$ 15.1 Water 84.9	1.1	28.2	Chlor benzene 50 Silicon oil 50	5. 46	Benzylic alcohol 89 CCl_4 11	3.6
5	$NaNO_3$ 15 Water 85	1.1	25.6	Chlor benzene 85 Silicon oil 15	1.40	Benzylic alcohol 89 CCl_4 11	3.5
6	$NaNO_3$ 14.9 Water 85.1	1.1	22.8	Chlor benzene 92 Silicon oil 8	1.03	Benzylic alcohol 89 CCl_4 11	3.6

In Table 2, we give the experimental parameters for three different cases of drop dynamics, under various surface tension gradients Π. The first case (systems 1 and 2) corresponds to the undeformable drops (Fig. 8). The second case (systems 3 and 4) represents the situation of the deformable drops (Fig. 9) and the third one (Fig. 10) describes the break-up of a drop.

Also, Table 2 gives the composition of the continuous (L) bulk and drop (L') phases, as well as the surfactant phase description and various phase physical characteristics. The continuous liquid bulk phase (μ) and drop phase (μ') viscosities and the interfacial tension, σ_0 and σ_1, values are also given in Table 2. Investigated drops have the radius comprised between 0.46 and 1.19 cm.

Table 3.

Surface tension gradients, $\Pi = \sigma_0 - \sigma_1$, the ratio of the viscosities, λ, and the calculated values of Marangoni hammer force $F_M(0)$, for the six systems given in Table 2.

Sys-tem	Π (dyn/cm)	λ	$F_M(0)$, (dyn)	Remarks
1	4.4 ± 0.3	35.39	2.71	The free drop remains undeformable, having, at most, surface waves, as in Fig. 8.
2	6.7 ± 0.3	60.15	2.45	
3	25.1 ± 0.3	7.31	26.15	The free drop might have slight or big deformations, but after 0.6-0.8 sec., it returns to its initial form, as in Fig. 9.
4	24.6 ± 0.3	4.96	35.77	
5	22.1 ± 0.3	1.27	84.31	The free drop, after 0.3-0.4 sec., breaks up into two drops, as shown in Fig. 10.
6	19.2 ± 0.3	0.94	85.70	

The values of the surface tension gradient, Π, the ratio of the viscosities $\lambda = \mu'/\mu$ and the Marangoni hammer $F_M(0)$ force (see, equation 30) are given in Table 3.

Then, we compare the calculated values, obtained with our hydrodynamic theoretical model, with some experimental observations on the deformations and the break-ups of the drops under the surface tension gradient. The drops were visualized by filming with a high-speed camera

(500 images/sec). A number of image sequences illustrating the deformations of the drop at various moments (at different times, t) are presented in Figs. 9 and of the break-up in Figs. 10.

In Fig. 8, the filmed drop images, at different moments of time (t), are shown for the case of an undeformable free drop. In these images is possible to observe the motion of the surfactant front on the drop surface, easily distinguishable, by the contrast with the uncovered drop surface. Also, in Fig. 8, we can observe that the horizontal line, corresponding for the initial position of the free drop, is only slightly modified in time and the drop is not deformed or moved.

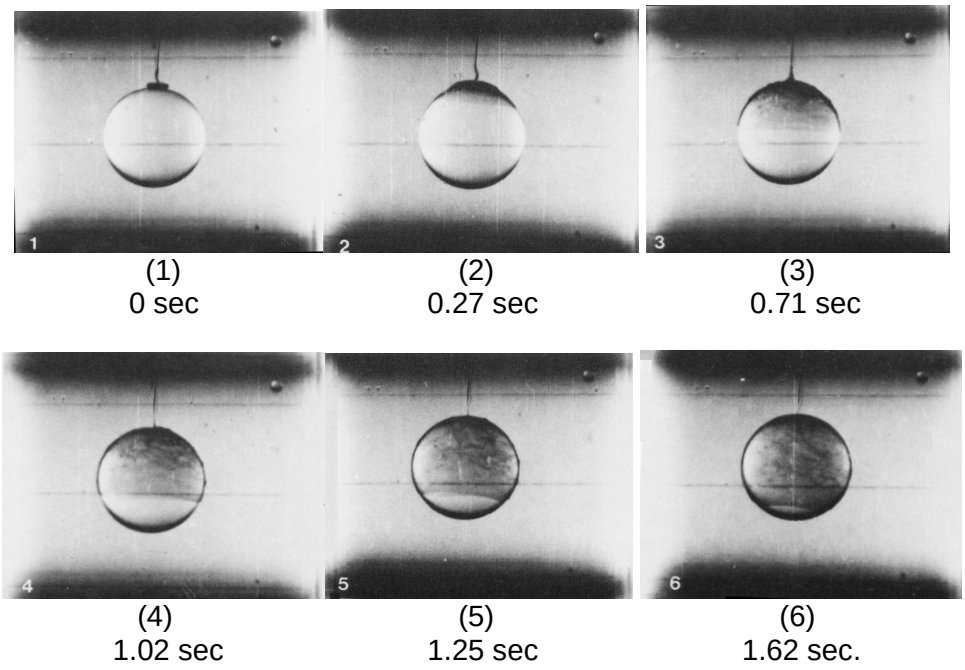

Fig. 8. Filmed pictures of an undeformable drop characterized by the system 2, given in Tables 2 and 3; the interfacial tension difference, $\Pi = \sigma_0 - \sigma_1 = 6.7$ dyn/cm, the viscosities ratio $\lambda = 60.15$ and the calculated Marangoni force $F_M(0) = 2.45$ dyn.

These findings are in substantial agreement with the data earlier published [3], for non-deformable free drops. For comparison, we have chosen similar experimental conditions given in Table 2, and therefore, we clearly demonstrated the reproducibility of these experiments. In plus, here, we calculated the Marangoni force $F_M(0)$, see Table 3.

Fig. 9 shows different shapes of a deformable free drop and its movement from the initial position (i.e. from the shown reference horizontal

line). In this case, for the system 4, given in Tables 2 and 3, due to the variation of the drop shape, besides the Marangoni force, the surface dilution and capillary forces will appear in the description of drop deformation.

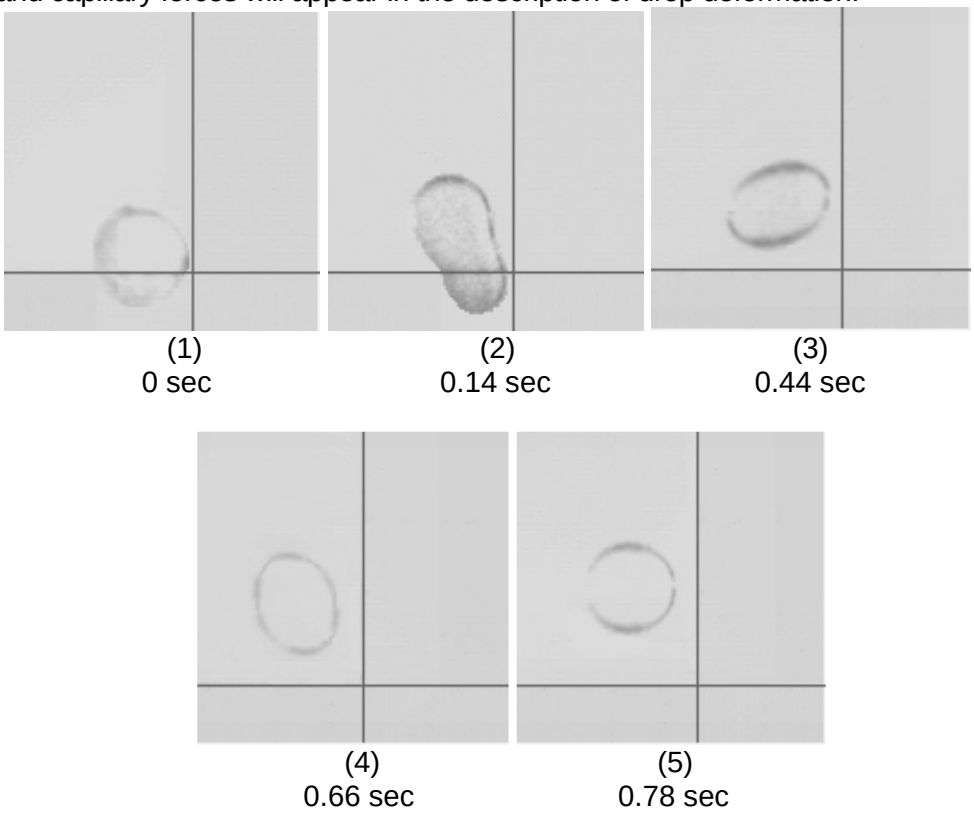

Fig. 9. Filmed pictures of drop deformations. The liquid-liquid system is characterized by the system 4 in Tables 2 and 3; Π=24.6 dyn/cm; λ = 4.96; $F_M(0)$ = 35.77dyn.

Fig. 10 illustrates the drop deformations (panels 1, 2 and 3), the drop movement and the break-up (panel 4, 5 and 6) of the drop into two parts. This is the third case of a deformable drop observed for the system 6, and its detailed characterization is given in Tables 2 and 3. It can be seen that at a certain moment in time (Fig. 10, panel 5) a tip in one of the drop compartments appears. Fig. 10, panel (5), might be an example of the tip-stretched effect.

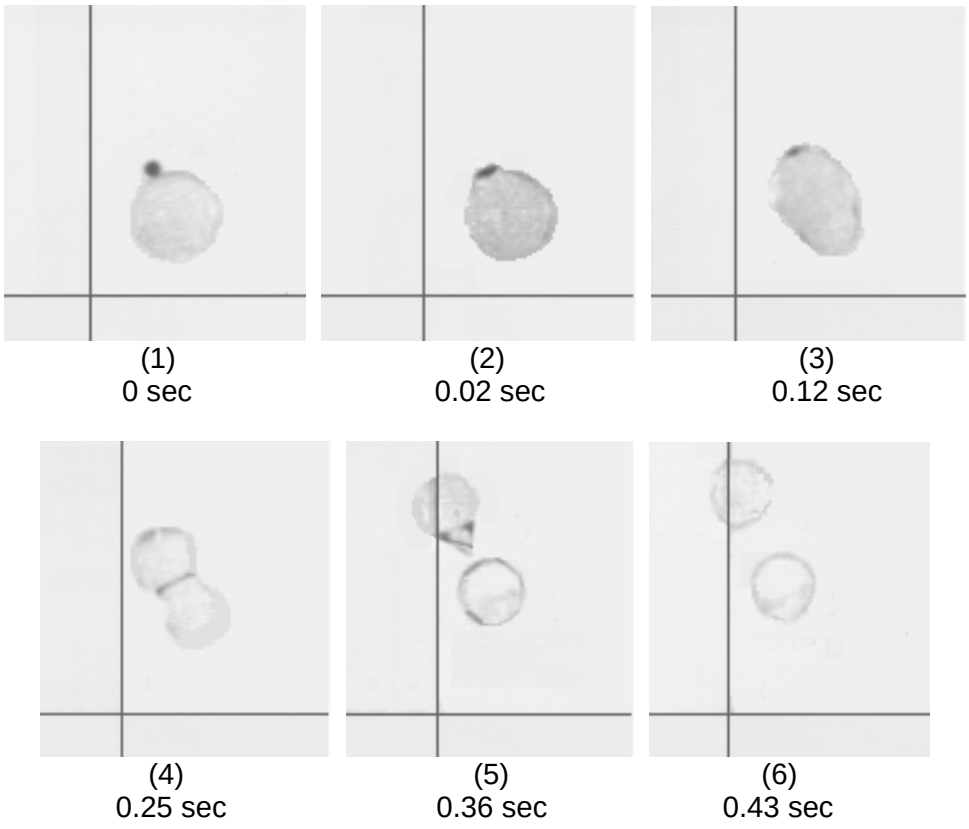

Fig.10. Filmed pictures of the initial free drop (a), the deformed drop (b) and the breakup drop (c). The liquid/liquid system is characterized by the system 6 given in Tables 2 and 3; Π = 19.2 dyn/cm; λ = 0.94; $F_M(0)$ = 85.70 dyn.

As we can see, from Table 3, for systems 1 and 2, the values of viscosities ratio, $\lambda >> 1$, are very large, and the values of the Marangoni force, F_M (0), are slightly smaller than 3 dyn, and the drop is non deformable (Fig. 8). For systems 3 and 4, given in Table 3, the ratio values of the bulk viscosities are greater than unity $\lambda > 1$ (Table 3) and the Marangoni force is much higher than 1.

The Fig. 9 presents the different shapes of the free drop dynamics. Because there is a variation of the drop shape, in this case, the surface dilution and capillary forces will appear. This is the situation of a slightly viscous drop, when the Marangoni effect will provoke the drop deformations, which will generate the surface dilution in parallel with the appearance of capillary forces (Fig. 9, panel 2).

For the system 6, described in Tables 2 and 3, the viscosity of continuous bulk (μ) liquid and of the drop (μ') liquid are almost equal, $\lambda \approx 1$,

Table 3, but the Marangoni force $F_M(0)$ takes the highest value. In this situation, after a few moments (about 0.36 sec) the break-up of the drop appears (Fig. 10, panel 5), and the drop is divided into two parts (droplets).

This is the most complicated situation, when the Marangoni force will provoke the drop deformations, which will generate, in parallel, the surface dilution and the tip-stretching, until the drop is broken into two drops, as illustrated in Fig. 10, panel 5.

CONCLUSION

A hydrodynamic model has been developed in which the variable interfacial tension at the well defined free drop surface, caused by the addition of a surfactant, will generate a Marangoni force primarily responsible for the drop deformations and movements.

The drop deformation process is described and analyzed mathematically. It has been shown that it is a deep dependence of the absolute values of the Marangoni force $F_M(0)$ and the deformations of a free drop. In other words, a small Marangoni force will not cause the deformations of the viscous drop, but a large Marangoni force will provoke complicated deformations and movements of a free drop even the break-up of the drop. Thus, it is also shown experimentally and theoretically that the Marangoni force is a primary cause of the deformations of a drop. Surface dilution and tip-stretching effects, as well as the capillary forces, might appear as secondary factors in the drop deformation processes.

When a surface tension gradient appears at the free drop surface, the hammer Marangoni force $F_M(0)$ determines primarily the drop deformations and movements, taking into account the physical characteristics of the continuous liquid bulk phase and of the drop liquid phase, as well as those for the chosen surfactant solutions as indicated in Tables 2 and 3.

We can conclude that we explored six experimental systems that are classified into three important cases, in substantial agreement with the data given in Table 3. When the Marangoni hammer forces are small, the drop shape is not modified. For the intermediary values of the Marangoni hammer forces the drop is deformable. At the high values of Marangoni hammer forces the drop breaks up into two or more droplets.

Further, Marangoni hammer forces can also generate other different effects, like the surface dilution and the tip-stretching, as well as the capillary forces, that might appear in the drop dynamics, depending on the working conditions.

Finally, it is to be emphasized that such phenomena, generated by Marangoni force and Marangoni instability, are a result of the adsorption of a surfactant at the surface between the two liquid phases. These phenomena are of a major interest, both in industrial and biological

processes, in movements at biological membranes, as well as in the space science and technology of liquids.

REFERENCES

1. E. Chifu, "Surface flow of liquids in the absence of gravity", proposal selected by NASA's Office of Aeronautics and Space Technology, 1977, pp. 1-39.
2. E. Chifu and I. Stan**,** *Rev. Roum. Chim.,* **1980**, *25*, 1449-1459.
3. E. Chifu, I. Stan**,** Z. Finta and E. Gavrila, *J .Colloid Interface Sci.,* **1983**, *93*, 140-150.
4. I.Stan, E. Chifu, Z. Finta and E. Gavrila, *Rev. Roum. Chim.,* **1989***, 34*, 603-615.
5. I.Stan**,** C.I. Gheorghiu and Z. Kasa, *Studia Univ. Babes- Bolyai, Math.,* **1993**, *38*(2), 113-126.
6. E. Chifu, I. Albu, C. I. Gheorghiu, E. Gavrila, M. Salajan and M. Tomoaia-Cotisel, *Rev. Roum. Chim.,* **1986**, *31*, 105-112.
7. I.Stan, E. Chifu and Z. Kása, *ZAMM, Z. angew. Math. Mech.,* **1995**, *75*, 369-370.
8. M. I. Salajan, A. Mocanu and M. Tomoaia-Cotisel, "Advances in Thermodynamics, Hydrodynamics and Biophysics of Thin Layers", University Press, Cluj-Napoca, **2004,** pp. 1-117.
9. E. Chifu, I. Stan and M. Tomoaia-Cotisel, *Rev. Roum. Chim*., **2005,** *50*, 297-303.
10. M. D. Levan, *J. Colloid Interface Sci*., **1981**, *83*, 11-17
11. L. Landau and E. Lifschitz, "Mécanique des fluides*",* **1971,** Ed. Mir, Moscou.
12. V. G. Levich, "Physicochemical Hydrodynamics*"*, Chap. VIII. Prentice-Hall, Englewood Cliffs, New Jersey, **1962.**
13. T. Oroveanu, Mecanica fluidelor vâscoase*,* Ed. Acad., Bucharest, **1967.**
14. L. E. Scriven, *Chem. Eng. Sci.,* **1960**, *12*, 98-108.
15. R. Aris, "Vectors, Tensors and the Basic Equations of Fluid Mechanics*"*, Chap. X. Prentice-Hall, Englewood Cliffs, New Jersey, **1962**.
16. A.Sanfeld, in "Physical Chemistry Series*"*, (W. Jost, Ed.), Vol. I, Acad. Press, New York, **1971**.
17. I.R. Stan, M. Tomoaia-Cotisel and A. Stan, *Bull. Transilvania Univ. Brasov,* **2006***,13*(48) 357-367
18. A.Wierschem, H. Linde and M. G. Velarde, *Phys. Rev. E.,* **2000**, *62*, 6522-6531
19. Y. T. Hu and A. Lips, *Phys. Rev. Lett.*, **2003**, *91*, 1- 4
20. H. A. Stone and L. G. Leal, *J. Fluid Mech.,* **1990**, *220*, 161-186
21. W. J. Milliken, H. A. Stone and L. G. Leal, *Phys. Fluids,* A, **1993**, *5*, 69-79
22. A.D. Eggleton and K. J. Stebe, *J. Colloid Interface Sci.,* **1998**, *208*, 68-80.
23. R. Savino R. Monti, F. Nota, R. Fortezza, L. Carotenuto C. Picolo, *Acta Astronautica,* **2004**, *55*(3), 169-179.